PROCEEDINGS OF SCIENCE

Unveiling the origin of cosmic-ray leptons within a coherent multi-channel propagation scenario

Ottavio Fornieri[*†]
Department of Physical Sciences, Earth and Environment, University of Siena,
Via Roma 56, 53100 Siena, Italy
INFN Sezione di Pisa, Polo Fibonacci, Largo B. Pontecorvo 3, 56127 Pisa, Italy
Instituto de Física Teórica UAM-CSIC, Campus de Cantoblanco, E-28049 Madrid, Spain
E-mail: ottavio.fornieri@pi.infn.it

Daniele Gaggero
Instituto de Física Teórica UAM-CSIC, Campus de Cantoblanco, E-28049 Madrid, Spain
E-mail: daniele.gaggero@uam.es

Dario Grasso
INFN Sezione di Pisa, Polo Fibonacci, Largo B. Pontecorvo 3, 56127 Pisa, Italy
E-mail: dario.grasso@pi.infn.it

The interpretation of cosmic-ray (CR) data still represents a significant challenge: a coherent interpretation of the measured CR spectra is hampered by our incomplete knowledge about both the acceleration mechanisms and the transport properties across the Galaxy. The main challenge in this context is to identify a unified picture that includes all the available observables. To this aim, we first perform a multi-channel fit of the available CR data based on the DRAGON numerical code, to set the relevant propagation parameters. Then, we discuss several physically-motivated possibilities (*i.e.* recent burst, constant-luminosity, time-dependent emission) for the injection of e^+e^- pairs accelerated at nearby antimatter factories, such as pulsar wind nebulae, and compute their propagation. Finally, we address the all-lepton spectrum and assess the contributions of both young, nearby supernova remnants, and possibly an additional hidden source, to the observed CR lepton flux above ~ 1 TeV recently measured by H.E.S.S., VERITAS, CALET and DAMPE.

36th International Cosmic Ray Conference -ICRC2019-
July 24th - August 1st, 2019
Madison, WI, U.S.A.

[*]Speaker.
[†]Corresponding author.

PoS(ICRC2019)068

1. Introduction

The origin and transport properties of leptonic cosmic rays (CRs) have intrigued scientists for decades. The achieved accuracy in the measurement of their spectrum offer valuable clues on the source ages/positions as well as on the details of the transport. Ground-based and space-born experiments have recently provided data on the e^+, e^- and $e^+ + e^-$ spectrum up to $\sim \mathcal{O}(10)$ TeV and have revealed several features: in particular, AMS-02 confirms the old issue known as *positron excess* [1], while CALET [2] and H.E.S.S. [3] observe a drop-off in the e^- and $e^+ + e^-$ spectrum after ~ 1 TeV. It is therefore challenging to connect these observed features to physics arguments. Here, we investigate whether nearby old cosmic accelerators such as supernova remnants (SNRs) and relatively young pulsar wind nebulae (PWNe) can explain those experimental results in the framework of a large-scale CR transport setup tuned on the most updated CR nuclei data. For the extended version of the results presented we refer to the principal paper [4].

2. The propagation setup: DRAGON computation of the large-scale CR component

The starting point for a phenomenological treatment of the problem is the transport equation that effectively captures CR diffusion in space and momentum, energy losses, advection, nuclear spallation and decays [5]. We solve it numerically with the DRAGON code[1] for the relevant CR species. For each one, an injection spectrum is modeled as a broken power-law in rigidity, propagating in a continuous-source 2D distribution — cylindrical symmetry — according to [6]. Isotropic diffusion is assumed, characterized by a scalar diffusion coefficient scaling as $D_{xx}(p) = D_0 \left(\frac{\rho}{\rho_0}\right)^{\delta}$, where $D_0 \equiv D(\rho_0)$ is the normalization at reference rigidity $\rho_0 = 1$ GV. For the specific form of the transport equation that we use, details on how we treat reacceleration, hadronic and leptonic energy losses, and spallation, including the origin and meaning of each term, we refer to the DRAGON technical paper [7]. Throughout this work the gas density, magnetic and interstellar radiation-field distributions are fixed (with their own uncertainties) on the basis on astronomical data. On the other hand, CR injection spectra and diffusion parameters are largely unknown and have to be settled by comparing DRAGON predictions with CR data.

We use here AMS-02 data for CR protons [8] and heavier nuclei [9], and for the B/C ratio [10], complemented with Voyager data [11] for low energy protons and other nuclei outside the Heliosphere (unmodulated). AMS-02 data [12, 1] are also compared with the leptonic component. The results of the DRAGON predictions are shown in the panels of Figure 1.

The observed proton (heavier nuclei) spectra are reproduced with an injection index at low energy $\Gamma_{\rm inj} = 1.8$ ($\Gamma_{\rm inj} = 2.0$), a low-energy break at 7 GeV/n (for all species), an injection at intermediate energies $\Gamma_{\rm inj} = 2.4$ ($\Gamma_{\rm inj} = 2.3$), a high-energy hardening at 335(165) GeV/n and a high-energy injection $\Gamma_{\rm inj} = 2.26$ ($\Gamma_{\rm inj} = 2.15$). The B/C ratio is matched for a value of δ close to 0.45 and small re-acceleration ($v_{\rm A} = 13$ km/s). Primary electrons are injected with a hard spectrum ($\Gamma_{\rm inj} = 1.6$) up to the same break energy ($E_{\rm br} = 7$ GeV) and then with an index steeper than that of the other primary species ($\Gamma_{\rm inj} = 2.7$) due to synchrotron losses occurring before their release into the ISM. Regarding secondary positrons, the propagated spectrum at Earth computed with DRAGON is fixed by the proton and nuclei spectra, hence within the same transport setup.

[1] https://github.com/cosmicrays/DRAGON

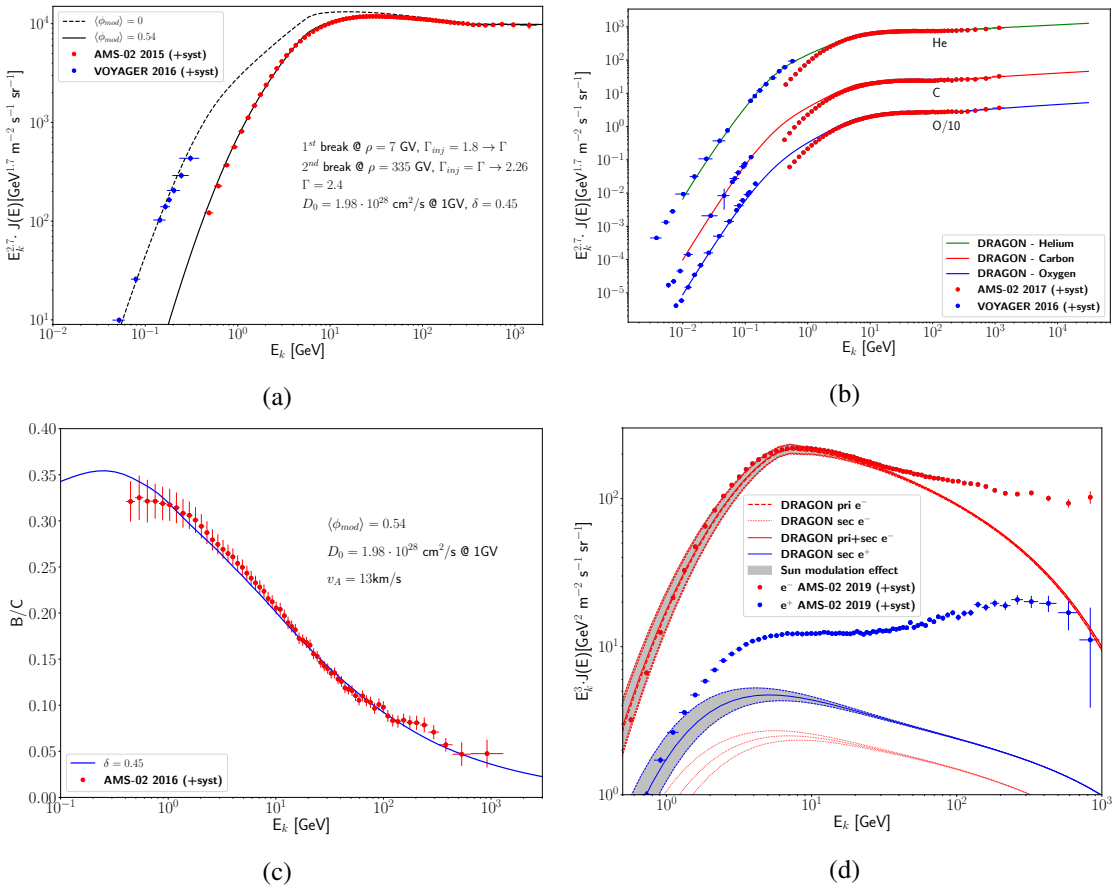

Figure 1: DRAGON propagated spectra, computed with our reference model, of (a) protons, (b) Helium, Carbon and Oxygen, compared with AMS-02 (sun modulated) and Voyager (interstellar) data. (c) B/C ratio computed for the same model and plotted against AMS-02 data. (d) Primary and secondary production of $e^{\pm}$. The silver band accounts for the solar modulation $\langle \phi_{mod} \rangle = 0.54 \pm 0.10$, estimated according to [13].

In accordance to what was already pointed out with the first release of the PAMELA data [14], we find (see Figure 1d) that above few GeV the positron flux is much steeper than expected: this issue is commonly referred to as *positron excess*. A similar statement holds for the electron flux. Even though new propagation paradigms or exotic scenarios involving new physics (such as dark matter annihilation) may be invoked to account for the unexpected production of positrons (see for instance [15] and references therein), pair-emission from pulsar wind nebulae (PWNe) seems to be a more natural candidate. We will assess their contribution in the next section.

3. Treating the positron excess: basics from PWN acceleration and relevant caveats

Pulsar wind nebulae are structures found inside the shells of supernova remnants, which emit a broad-band spectrum of non-thermal radiation powered by a fast-spinning magnetized neutron star with a typical radius $R \sim 10$ km and periods of $\mathcal{O}(0.1 - 10)$ s, typically detected in the radio and/or gamma-ray band as *pulsars*. In order to characterize the emission from a PWN, it is important to assess: **1)** the energy release as a function of time, and **2)** the acceleration mechanisms of

the electron+positron pairs, hence the energy spectrum of such leptons when they are eventually released in the interstellar medium (ISM).

1. The slowing-down of the pulsar rotation can be described by $\dot{\Omega}(t) = -\kappa_0 \cdot \Omega(t)^n$, where $\Omega(t) = P^{-1}$ is the rotation frequency, κ_0 and n are parameters that depend on the specific energy-loss process; n is commonly called *braking index*. This equation can be solved to get $\Omega(t)$ and the time evolution of the luminosity, which can be written as follows:

$$L(t) = I\Omega(t)\dot{\Omega}(t) = \frac{\eta^{\pm} L_{0,\gamma}}{\left(1+\frac{t}{\tau_0}\right)^{\frac{n+1}{n-1}}} \tag{3.1}$$

   where $\eta^{\pm}$ is the conversion efficiency of the released energy into $e^{\pm}$ pairs and we have defined $\tau_0 \equiv \frac{1}{(n-1)\kappa_0 \Omega_0^{n-1}}$. Here, t is the characteristic age of the source ($t_{\rm ch} \approx \frac{P}{(n-1)\dot{P}}$), provided that the diffusive time ($t^* \equiv t^*(E)$) needed for a particle to travel from the source to the Earth is much smaller than the age itself, which is true for nearby ($d \sim \mathcal{O}(100)$ pc) sources of high-energy leptons ($\mathcal{O}(100)$ GeV).
   Equation (3.1) is purely observational and, as long as κ_0 and n are not specified, does not involve any underlying model. τ_0 is a timescale for the luminosity function and it affects the injection from the source into the ISM. In fact, if $t \ll \tau_0$, we can Taylor-expand (3.1) as $L(t) \approx \eta^{\pm} L_{0,\gamma}(1 - \frac{n+1}{n-1} \cdot t/\tau_0)$ and approximate the injection as a constant over time. If instead $t \gg \tau_0$, the luminosity drops dramatically with time and we can approximate the injection with an instantaneous burst.

2. The current data on the non-thermal radiation (in *Radio* and *X-ray* frequencies) emitted from several well-observed PWNe [16] require a lepton spectrum which has the shape of a broken power law, with a hard spectrum (with slope $1 \lesssim \Gamma_{\rm inj} \lesssim 2$) below a break at $\sim 200 - 400$ GeV, and a steeper one ($\Gamma_{\rm inj} > 2$) at larger energies (see [17]). The low-energy spectrum has been debated over the years, and several acceleration mechanisms were proposed (*e.g.* magnetic reconnection at the termination shock and resonant absorption of ion-cyclotron waves).

If we assume that the bulk of energy loss by a pulsar is due to magnetic-dipole (MD) emission, than $\tau_0^{\rm MD} = \frac{3Ic^3}{B^2 R^6 \Omega_0^2}$ and $n = 3$ [18]. With this assumption, the nominal parameters tabulated in the ATNF Catalogue[2] for the nearby (within ~ 2 kpc) pulsars give $t_{\rm ch}/\tau_0 \sim \mathcal{O}(10^{-1})$, favoring the constant-luminosity injection scenario. On the other hand, measurements on the braking index of isolated pulsars [19] give values $1.9 < n < 2.8$, which is significantly less than the MD prediction. Plus, the constant-luminosity case is in contrast with the treatment that many authors give for the problem, due to both physical assumptions and fits of the data (see for instance [20]).

For this reason, in what follows we will explore both scenarios for the positron flux.

3.1 Contribution from old and young pulsars: study of the analytical solution of the transport equation

The HAWC Collaboration recently detected an extended (~ 20 pc) gamma-ray halo in the TeV range around two nearby (~ 300 pc) known pulsars, Monogem and Geminga [21]. Due to their

[2] http://www.atnf.csiro.au/people/pulsar/psrcat/

close distance and following the lead of the previous literature, we parametrize the problem of the positron excess above ~ 40 GeV considering the missing e^+ coming from either one or the other.

We describe the transport process with a simplified version of the transport equation, where low-energy effects such as advection and re-acceleration are neglected and spherical symmetry is assumed. This equation and its analytical solutions are discussed in detail in [20], where they are treated in the two limiting cases of constant-luminosity and burst-like injection, and in the general continuous-luminosity case described by (3.1). It is very instructive to show the behavior of the propagated spectrum in this latter general case, Figure 2.

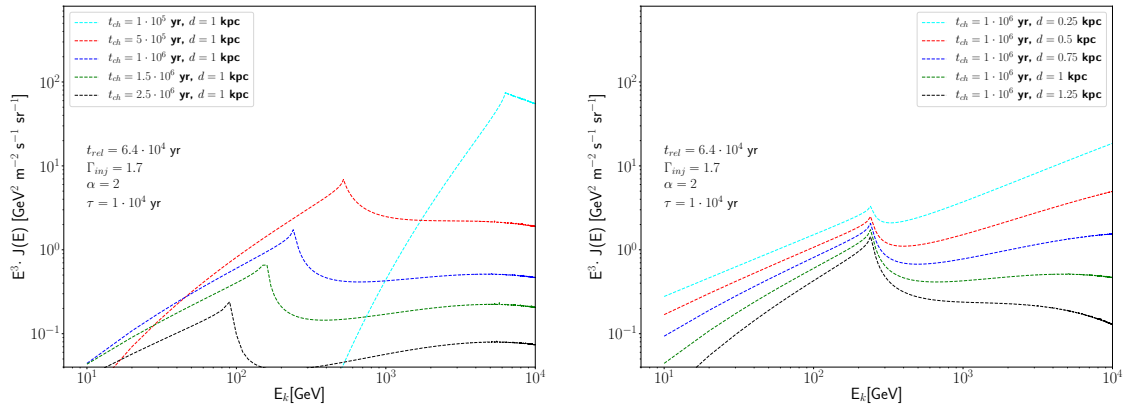

(a) (b)

Figure 2: Solution of the transport equation for a decaying-luminosity single-source, plotted for objects of (a) different ages and fixed distance (1 kpc) and (b) different distances and fixed age ($1 \cdot 10^6$ yr). The injection index is $\Gamma_{\rm inj} = 1.7$, although we verified that the shifting is independent of it.

The peak in the propagated spectrum shifts towards lower energies as the age of the source increases. Its position is found solving the equation for the rate of energy loss $\frac{dE}{dt} \simeq -b_0 E^2$, unless additional features at the injection are considered, $E_{\rm peak}(t) = \min\left\{\frac{1}{b_0(t-t_{\rm rel})}, E_{\rm feat}\right\}$, where t is the age of the source and $t_{\rm rel}$ the time it takes for particles to leave the source region.

For these reasons, we expect the low-energy range (below ~ 40 GeV) of the positron flux to be given by the convolution of a large ($\mathcal{O}(10^4)$ within ~ 7 kpc) number of old ($t_{\rm age} > 10^6$ yr) PWNe. These numbers are compatible with the SN explosion rate in the Galaxy.

3.2 Bayesian fits to the positron flux

DRAGON is able to implement the above-mentioned convoluted spectrum propagating a smoothly injected ($\Gamma_{\rm inj} = 2.28$) so-called *extra-component*. On top of this, plus the secondary $e^\pm$ component, we fit the contribution of young nearby sources in four different scenarios, resulting from the combination of burst-like or constant-luminosity release with a break or a cut-off at the injection. The fit is based on AMS-02 data [1] above 20 GeV, to bypass the solar modulation.

For reasons due to age and total-energy injected in the ISM, the two limiting cases require the main contributor to switch between Geminga and Monogem. We implement our theoretical knowledge of the problem setting priors in the injection spectrum ($\Gamma_{\rm inj} \in [1,2]$) and in the position of the feature ($E_{\rm cut,\ break} > 150$ GeV). For illustrative purposes, here we only show the case with constant luminosity and a broken power-law.

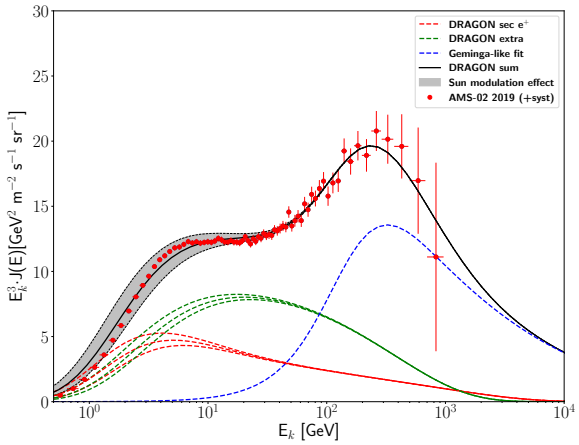

Figure 3: Bayesian fit to the positron flux where constant-luminosity injection and a broken power-law are implemented in the following fit function: $S(E) = S_0 \left(\frac{E}{E_0}\right)^{\Gamma_{\rm inj}} \cdot \left(1 + \left(\frac{E}{E_{\rm break}}\right)^{|\Delta\Gamma_{\rm inj}|\cdot s}\right)^{{\rm sign}(\Delta\Gamma_{\rm inj})/s}$.

The resulting spectrum is very hard ($\Gamma_{\rm inj} \simeq 1.1$) below the break energy ($E_{\rm break} \simeq 160$ GeV) and softer ($\Gamma_{\rm inj} \simeq 2.8$) above. This values are compatible (within the uncertainties) with the mentioned theoretical predictions. We also find similar outcomes for the other three cases.

4. Local electron accelerators explain the high-energy electron data

Due to the overall contribution of e^- with respect to e^+, once the latter are assessed by means of antimatter factories, sources of electrons only are still needed.

Multi-wavelength observations show the presence of five SNRs in the local region (within ~ 1 kpc) surrounding the Earth[3], identified with the names Vela Jr, Vela, Cygnus Loop, Simeis-147, IC-443. A bayesian fit of these sources is performed in [4], based on AMS-02 [22] plus H.E.S.S. [3] all-lepton data, showing that, neglecting the rigid contribution of H.E.S.S. systematics, an additional SNR source is needed to reproduce the ~ 1 TeV feature. To characterize this source we perform a bayesian fit of the same data set in the two limiting cases where **1)** no known SNRs are present, **2)** all the known SNRs are present. We parametrize the source as a featureless injection with a luminosity function $L(t) = \frac{L_0}{\left(1+\frac{t}{\tau_{\rm d}}\right)^{\alpha_{\rm d}}}$. Here $(\alpha_{\rm d}, \tau_{\rm d})$ capture the release from the shock, a process still under debate, therefore they are parameters of the fit. A prior is set on the injection index to be $\Gamma_{\rm inj} \in [1,2]$, based on the *diffusive-shock-acceleration* assumption [23]. The outcome of this procedure is shown in Figure 4.

As a result of this analysis, we find that a hidden old remnant of $\sim 10^5$ yr is needed to reproduce the data, and the best-fit distance is expected to be in the range (600 – 1200) pc.

5. Conclusions

In this work we provided a comprehensive setup to reproduce the most relevant features observed in the positron, electron and all-lepton data recently released by the AMS-02, CALET, and

[3] `http://www.physics.umanitoba.ca/snr/SNRcat`

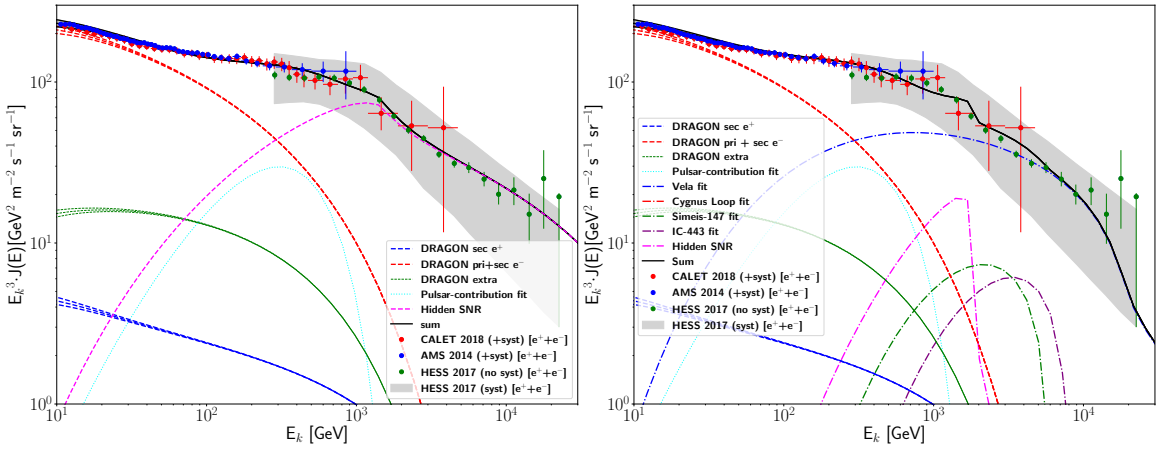

(a) (b)

Figure 4: Bayesian fit of a hidden source potentially responsible for the all-lepton flux. The secondary and primary production, the extra-component and the fitted pulsar contribution, are considered as background.

H.E.S.S. collaborations. With a properly set propagation model, we find a distance range (600 – 1200 pc) where to search for a hidden old SNR. This range is different from the value quoted in [24], where a close source ($d = 100$ pc) is invoked to match the observed data. The discrepancy is mainly due to the propagation setup: we find that, in accordance with [24], such a close source would correctly reproduce the data only if a diffusion coefficient with a Kolmogorov-like rigidity-scaling ($\delta = 0.33$) and a smaller normalization were assumed. We remark that our reference transport scenario with $\delta = 0.45$ is compatible with the MCMC analysis carried out in [25].

References

[1] M. Aguilar *et al.* AMS Collaboration, *Towards Understanding the Origin of Cosmic-Ray Positrons*, *Phys. Rev. Lett.* **122**, 041102.

[2] O. Adriani *et al.*, *Extended Measurement of the Cosmic-Ray Electron and Positron Spectrum from 11 GeV to 4.8 TeV with the Calorimetric Electron Telescope on the International Space Station*, *Phys. Rev. Lett.* **120**, 261102 (2018).

[3] D. Kerszberg, *The cosmic-ray electron spectrum measured with H.E.S.S.*, *International Cosmic Ray Conference, [CRI215]* (2017).

[4] O. Fornieri, D. Gaggero, D. Grasso, *Features in cosmic-ray lepton data unveil the properties of nearby cosmic accelerators*, [astro-ph/1907.03696].

[5] V. S. Berezinsky, S. V. Bulanov, V. A. Dogiel, V. S. Ptuskin, *Astrophysics of cosmic rays* Amsterdam, Netherlands: North-Holland, 1990.

[6] K. Ferriere, *The interstellar environment of our galaxy*, *Rev. Mod. Phys.* Volume **73**, Issue 4, pp. 1031-1066 [astro-ph/0106359].

[7] C. Evoli, D. Gaggero, A. Vittino, G. Di Bernardo, M. Di Mauro, A. Ligorini, P. Ullio, D. Grasso, *Cosmic-ray propagation with DRAGON2: I. numerical solver and astrophysical ingredients*, *JCAP* **02**, 015, 2017 [astro-ph/1607.07886].

[8] M. Aguilar *et al.* AMS Collaboration, *Precision Measurement of the Proton Flux in Primary Cosmic Rays from Rigidity 1 GV to 1.8 TV with the Alpha Magnetic Spectrometer on the International Space Station*, *Phys. Rev. Lett.* **114**, 171103.

[9] M. Aguilar *et al.* AMS Collaboration, *Observation of the Identical Rigidity Dependence of He, C, and O Cosmic Rays at High Rigidities by the Alpha Magnetic Spectrometer on the International Space Station*, *Phys. Rev. Lett.* **119**, 251101.

[10] M. Aguilar *et al.* AMS Collaboration, *Precision Measurement of the Boron to Carbon Flux Ratio in Cosmic Rays from 1.9 GV to 2.6 TV with the Alpha Magnetic Spectrometer on the International Space Station*, *Phys. Rev. Lett.* **117**, 231102.

[11] A.C. Cummings *et al.*, *Galactic Cosmic Rays in the Local Interstellar Medium: VOYAGER 1 Observation and Model Results*, *The Astrophysical Journal*, Volume **831**, Number 1.

[12] M. Aguilar *et al.* AMS Collaboration, *Towards Understanding the Origin of Cosmic-Ray Electrons*, *Phys. Rev. Lett.* **122**, 101101.

[13] I. G. Usoskin, K. Alanko-Huotari, G. A. Kovaltsov, K. Mursula, *Heliospheric modulation of cosmic rays: Monthly reconstruction for 1951-2004*, *Journal of Geophysical Research (Space Physics)*, Volume **110**, Issue A12, CiteID A12108.

[14] O. Adriani *et al.* PAMELA Collaboration, *An anomalous positron abundance in cosmic rays with energies 1.5-100 GeV Nature* Volume **458**, pages 607âĂŞ609.

[15] D. Gaggero, M. Valli, *Impact of cosmic-ray physics on dark matter indirect searches*, *Advances in High Energy Physics* Volume **2018**, Article ID 3010514, 23 pages, [astro-ph/1802.00636].

[16] F. Jankowski, W. van Straten, E.F. Keane, M. Bailes, E. Barr, S. Johnston, M. Kerr, *Spectral properties of 441 radio pulsars*, *Mon. Not. R. Astron. Soc.* **473** (2018) 4436-4458, [astro-ph/1709.08864].

[17] P. Blasi, E. Amato, *Positrons from pulsar winds*, [1007.4745].

[18] D. R. Lorimer, M. Kramer, *Handbook of Pulsar Astronomy*, Cambridge University Press, 2004.

[19] O. Hamil, J. R. Stone, M. Urbanec, G. Urbancová, *Braking index of isolated pulsars*, *Phys. Rev. D* **91**, 063007 (2015).

[20] A. M. Atoyan, F. A. Aharonian, H. J. Völk, *Electrons and positrons in the galactic cosmic rays*, *Phys. Rev. D* **52**, 3265 (1995).

[21] A. U. Abeysekara *et al.*, *Extended gamma-ray sources around pulsars constrain the origin of the positron flux at Earth*, *Science* Vol. **358**, Issue 6365, pp. 911-914.

[22] M. Aguilar *et al.* AMS Collaboration, *Precision Measurement of the (e^++e^-) Flux in Primary Cosmic Rays from 0.5 GeV to 1 TeV with the Alpha Magnetic Spectrometer on the International Space Station*, *Phys. Rev. Lett.* **113**, 221102.

[23] D. Caprioli, P. Blasi, E. Amato, M. Vietri, *Dynamical Effects of Self-Generated Magnetic Fields in Cosmic-Ray-modified Shocks*, *The Astrophysical Journal Letters*, Volume **679**, Number 2. [astro-ph/0804.2884].

[24] S. Recchia, S. Gabici, F. A. Aharonian, J. Vink, *A local fading accelerator and the origin of TeV cosmic ray electrons Phys.Rev. D* **99** (2019) no.10, 103022.

[25] Yuan, Qiang and Lin, Su-Jie and Fang, Kun and Bi, Xiao-Jun, *Propagation of cosmic rays in the AMS-02 era*, *Phys.Rev. D* **95** (2017) no.8, 083007.